Journal of Physics and Its Applications

Journal homepage : https://ejournal2.undip.ac.id/index.php/jpa/index

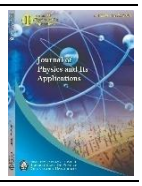

Photoluminescence effect on phosphorous irradiated zinc oxide (ZnO) nanotetrapods synthesized by simple thermal oxidation method

Bushra Aziz[1,3], Abdul Majid[2,3], Lubna Ghani[3*], Iffat Aziz[4]

[1]*Department of Physics, Women University of Azad Jammu & Kashmir, Bagh, Pakistan*
[2]*Department of Physics, Majmaah University, College of Science Al-Zulfi, Kingdom of Saudi Arabia*
[3]*Department of Chemistry, University of Azad Jammu & Kashmir, Muzaffarabad, Pakistan*
[4] *Department of Chemistry, Quaid.e.Azam University, Islamabad, Pakistan*

[*)]*Corresponding author: Lubnaghani41@gmail.com*

A R T I C L E I N F O

Article history:
Received: 25 June 2020
Accepted: 4 November 2020
Available online: 30 November 2020

Keywords:
ZnO
Tetrapods
Photoluminescence
Irradiation
Acceptor transition

A B S T R A C T

The irradiation effect on ZnO tetrapods was studied by Pelletron Tandem Accelerator at room temperature. ZnO tetrapods were synthesized by a simple thermal oxidation method by the vapors solid mechanism. The tetrapods were irradiated by phosphorous ion beam at different doses ($1x10^{14}$, $5x10^{14}$, $1x10^{15}$, $2.5x10^{15,}$ and $5x10^{15}$ ions/cm^2) having irradiation energy of 1MeV. After irradiation, these samples were characterized by scanning electron microscope (SEM), photoluminescence (PL), and energy dispersive spectrum (EDS). Photoluminescence (PL) spectra of our samples show that near band emission and deep level emission peaks increases with increasing dose and these emission peaks are defects related peaks. The PL spectra showed that the emission at 3.31eV and 3.26 eV attributed to a conduction band of phosphorus-related acceptor transition and a donor to the acceptor pair transition, respectively.

1. Introduction

Zinc oxide (ZnO), has gained much attention due to its multifunctional properties, such as chemical and photostability, the broad range of radiation absorption, and high electrochemical coupling coefficient making it attractive for potential use in electronics, optoelectronics, and laser technology [1-3].

Zinc oxide (ZnO) is a semiconductor material in material science, belonging to Group II-VI, its covalency lies between ionic and covalent semiconductor materials. Because of the presence of wide band-gap (3.37 eV), ZnO can be used in electromechanical nano devices, solar cells [4], gas sensors [5], sunscreen lotion (cream), cosmetic wounds healing, anti-hemorrhoids, anti-bacterial agent, eczema, and excoriation in the human medicine [6-7]. ZnO exist in different nanostructures such as nanowires [6-8], nanobelts [3], nanoneedles [9], oriented nanorods [10], nanowire-nanobelt arrays and nanoscale heterostructures [11], nanobridges and nanonails [12] but ZnO nanotetrapods (ZnO-T) structured materials have unique shape and structure [13–15], which considerably differ from other nanostructures. They have potential applications in photonics, lasing applications, and nano electronics [16–19]. Due to its high resistivity, ZnO is appropriate for applications of space and highly radiative environments likeaccelerators and atomic reactors. Due to the presence of native defects in ZnO such as zinc-vacancy (V_{Zn}), oxygen-vacancy (V_O), Zn interstitial (Zn_i), O at V_{Zn} (O_{Zn}), oxygen interstitial (O_i),and Zn at V_O (Zn_O)[20-22], it is a n-type semiconductor.

To getting reproducible and stable p-type still ZnO is a very difficult task because of the presence of deep acceptor levels,self-compensating process, and low dopant solubility. So, more attempts have alerted on producing p type ZnO materials. Elements of Group-V (N, P, As, and Sb) were widely reported for P-type ZnO [23]. Amongst the Group-V elements, the radius of nitrogen is close to the oxygen so it can be replaced at oxygen sites. This substitution produced no considerable modification in the ZnO lattice constant and phase. It gives both p and n-type ZnO, but n-type is dominant in more cases. Doping methods involve non-selective and non-localized doping procedures, which are required for device fabrication. An appropriate technique for doping and defects creating is ion irradiation, which provides the added advantages of lateral selectivity, an appropriate doping area, and fluence control. Many studies involving ions and electrons irradiation on ZnO revealed that the irradiation modifies the structural, optical, and electronic properties by creating shallow point defects [24–29]. Many researchers have successfully used the irradiation process to make phosphorous implanted P-type ZnO

thin films [30–32]. S. Nagar et al use Phosphorus irradiationat low energy (50 keV) on ZnO films that were grown by using a pulsed laser deposition technique. In short we can say that when ion beams irradiation pass through a target material, it produces numerous changes in the target material's properties. These changes depend upon the ion type, ions fluency, and ions energy. Different approaches are used to synthesize ZnO nanotetrapods structure, such as sol_gel, hydrothermal, arc discharge, vapor phase evaporation technique, chemical vapor deposition (CVD), laser ablation, and many others [33]. All these approaches used catalysts, expensive instrumentation, and toxic chemical which affect the cost and purity of the samples. So attempts always needed to introduce new low-cost approaches. Here we introduced a very simple method to synthesize ZnO nanotetrapods with highest purity in the presence of atmospheric oxygen at the temperature of 1000°C. This method is slightly modified from Vapor-phase growth technique [34], Thermal evaporation method [35], and Evaporation and recondensation method [36].

In this study we have synthesized Zinc oxide nanotatrapods (ZnO-T) structures using a simple thermal oxidation method and samples were then irradiated by phosphorus ions at different dose values. The morphology of the ZnO tetrapods was characterized by scanning electron microscope and studied the photoluminescence (PL) of the phosphorous irradiated ZnO nano-tetrapods (ZnO-T).

2. Experimental method

Due to low cost, simplicity, and high yield the simple thermal oxidation process was used for the synthesis of ZnO-tetrapod. No catalyst is needed in this process. Due to the high melting-point of ZnO high temperature is needed. In this method, simply metallic zinc (Zn) powder is placed directly in a ceramic boat and then put this boat in a vented electric furnace for 5 minutes which was already set at 1000ºC (This temperature should be above the boiling point of metallic Zn powder). Zn powder evaporates and reacts with atmospheric oxygen to form ZnO.After 5 minutes self-standing ZnO-tetrapods were obtained, cooled down until the furnace achieved room temperature, and collected. Before dispersing tetrapod on Si substrates, the substrates were cleaned by using a standard cleaning method. ZnO-tetrapods powder mixed with ethanol and then dispersed on Si substrates with the help of a centrifuge (500rpm) and dispersion were confirmed by SEM. The ion beam irradiation experiment was taken at the 5MV Pelletron Tandem accelerator. Five samples were prepared, then these samples were irradiated by Phosphorous ($p^{+\ +}$) ion beam at room temperature with an irradiation energy of 1Mev for different doses [($1x10^{14}$, $5x10^{14}$, $1x10^{15}$, $2.5x10^{15}$ and $5x10^{15}$) ions/cm^2]. The morphology of the unirradiated and irradiated samples was characterized by scanning electron microscope (SEM). The elemental analysis and the optical properties of the prepared ZnO-T samples were examined by the energy dispersive spectroscopy (EDS). photoluminescence (PL) spectroscopy respectively.

3. Results and discussion

Using a scanning electron microscope (SEM), the morphology of self-standing ZnO-tetrapods was observed. Before dispersing on substrates, the SEM image of ZnO-T were shown in Fig. 1. From this illustration, we can see that there are four arms interconnected at the same center and also have the same angle between arms. From the center, the four arms are thinner and at the end of the arms, it has needle-like sharp tips.

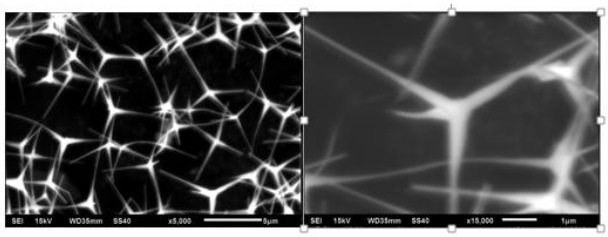

Fig. 1: SEM images of ZnOnanotetrapods (ZnO-T) (without substrate).

After dispersion on Si substrate and before Phosphorous ion beam implantation, the morphology and better distribution of the unirradiated ZnO-tetrapods on the substrate were examined with the help of SEM. Five samples (1,2,3,4, and e) was prepared which are shown in Fig. 2.

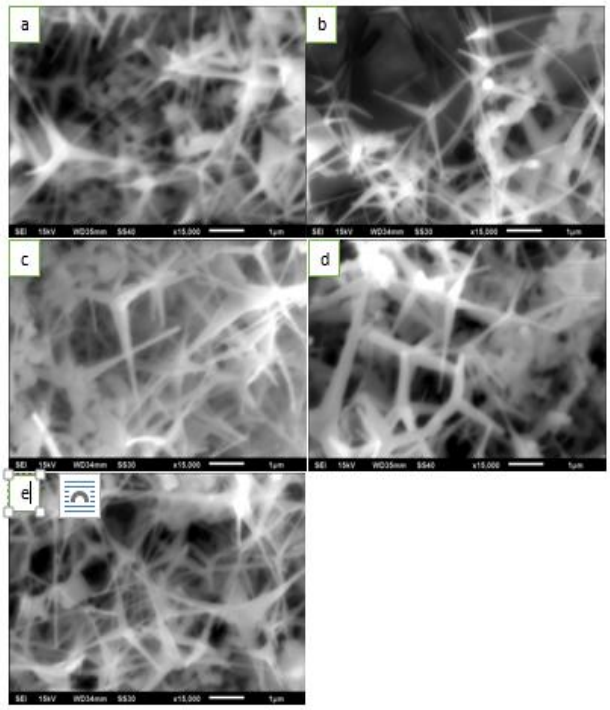

Fig. 2: SEM images of unirradiated sample 1 at a magnification of x15000 2(a) SEM images of unirradiated sample 2 at a magnification of x15000 2 (b) SEM images of unirradiated sample 3 at a magnification of x15000 2 (c) SEM image of unirradiated sample 4 at Magnification of x15000 2 (d) SEM images of unirradiated sample 5 at a magnification of x15000 2 (e).

Prepared samples were irradiated with phosphorous ion beam(P^{++}) with doses $1x10^{14}$, $5x10^{14}$, $1x10^{15}$, $2.5x10^{15}$ and $5x10^{15}$ ions/cm^2 respectively, 8 µc, 40 µc, 80 µc, 200 µc and 400 µc charges were deposited on sample 1, 2, 3, 4, and 5 respectively. Irradiated SEM images of ZnO-T samples were shown in Fig. 3. The arms of ZnO-

Tetrapods from the center to the wider point was long and thin along with the end of the arms are still sharp after implantation. There is no breaking of arms occurs in comparison with the unirradiated sample. So we can say that no significant effects were observed in ZnO-Tetrapods before and after phosphorous irradiation. The surface morphology of irradiated ZnO-Tetrapods was similar to the unirradiated ZnO-Tetrapods sample as reported earlier by Fang, Xuan Wang, Xiaohua et al in 2012 [2] and Lin, C.-C Chen, San-Yuan et al in 2004 [31].

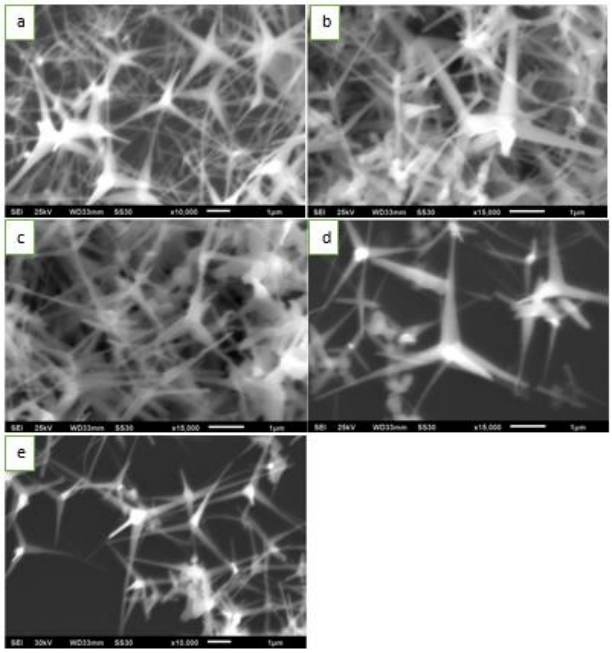

Fig. 3: SEM images of irradiated sample 1 with $1x10^{14}$ions/cm^2 at magnification of x10,000 3(a), SEM images of irradiated sample 2 with $5x10^{14}$ ions/cm^2 at magnification of x15000 3(b), SEM images of irradiated sample 3 with $1x10^{15}$ ions/cm^2 at magnification of x15000 3(c), SEM image of irradiated sample 4 with $2.5x10^{15}$ ions/cm^2 at Magnification of x15000 3(d), SEM images of irradiated sample 5 with $5x10^{15}$ ions/cm^2 at magnification of x10,000 3(e).

The optical properties of all the samples before and after irradiation with the phosphors were investigated by Photoluminescence (photon System Company). The wave length of the excitation source neon-copper (*NeCu*) laser used was 248 nm (5.0 eV). The PL spectrum of the control sample (unirradiated) is given in Fig. 4.

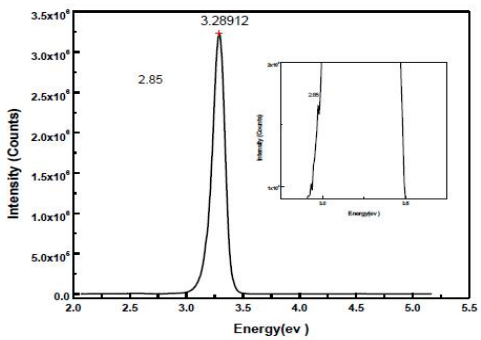

Fig. 4: PL spectra of unirradiatedZnO-Tetrapods controlled sample.

The inset graph shows the portion from 2.75 eV to 3.75. The spectrum is drawn between the PL intensity of the ZnOtetrapods sample and photon energy. The spectrum is fine and smooth. A narrow UV emission peak is seen at the energy of 3.28 eV (378 nm), which is induced by edge emission. The deep level emission (DLE) was found at 2.85 eV. When a dose of $1x10^{14}$ ions/cm^2 (8 μC charges) of Phosphorous given to the sample 1 then the uv emission peak of PL spectra is found at the energy of 3.31 eV, near band emission (NBE) and deep level emission (DLE) observed at the energies peak value 3.21 eV and 2.93 eV respectively. In sample 2 the dose of $5x10^{14}$ ions/cm^2 (charge of 40 μC) was used and on this dose or charge the uv emission peak found at 3.28eV, NBE, and DLE peak observed at energy value 3.23eV and 2.97eV respectively. In sample 3, 4 and 5 the doses of $1x10^{15}$ ions/cm^2 (charge of 80 μC), $2.5x10^{15}$ ions/cm^2 (charge of 200 μC) and $5x10^{15}$ ions/cm^2 (charge of 400 μC) were used respectively. On these dose values, the peak value of samples 3, 4, and 5 was 3.34 eV, 3.26 eV, and 3.28eV respectively. The NBE and DLE of samples 3 and 4 observed at energies of 3.30 eV, 3.22 eV, and 2.89 eV, 2.85 eV. For sample 5 the NBE was found at 3.26 eV and DLE at 2.89 eV. The PL spectra (DLE) of the unirradiated control sample, samples 1, 2, 3, 4, and 5 were shown in Fig 5. The full PL spectra peak is also illustrated in the inset of Fig. 5.

In irradiated PL spectra, the UV emission peaks at 3.31 eV can be ascribed to the free electrons to neutral-acceptor (FA) transition, whereas the emission peak located at 3.287 eV and 3.34eV is due to the donor-acceptor pair transition [29,30] and acceptor bound excitation (A^0 X) [37] respectively. This shows that phosphorous has an amphoteric behavior it forms both donor and acceptor states in ZnOnanotetrapods samples. It was also noted that irradiated ZnOnanotetrapods with Phosphorous doses of $5x10^{14}$, $1x10^{15}$, $2.5x10^{15,}$ and $5x10^{15}$ ions/cm^2 show a broad emission near band edge and deep level peaks. These broad emission peaks were created from different types of point defects, such as zinc interstitials (Zn_i) and oxygen vacancies (Vo). So on this discussion, it could conclude that more shallow defects will arises as the phosphorous dose increased.

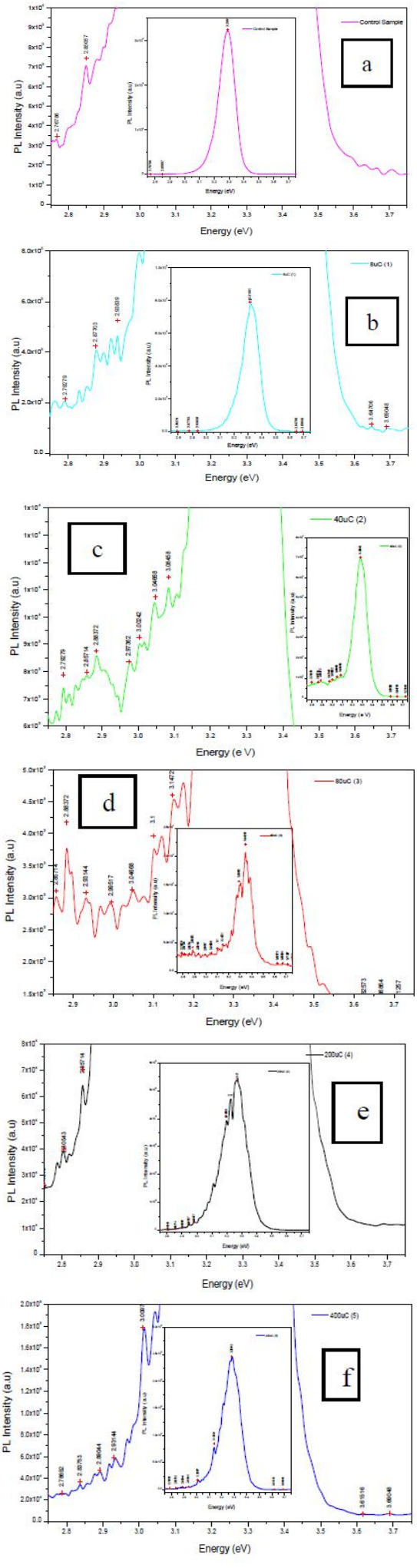

Fig. 5 PL spectra of control sample 5(a), PL spectra of irradiated sample 1 5(b), PL spectra of irradiated sample 2 5(c), PL spectra of irradiated sample 3 5(d), PL spectra of irradiated sample 4 5(e), PL spectra of irradiated sample 5 5(f).

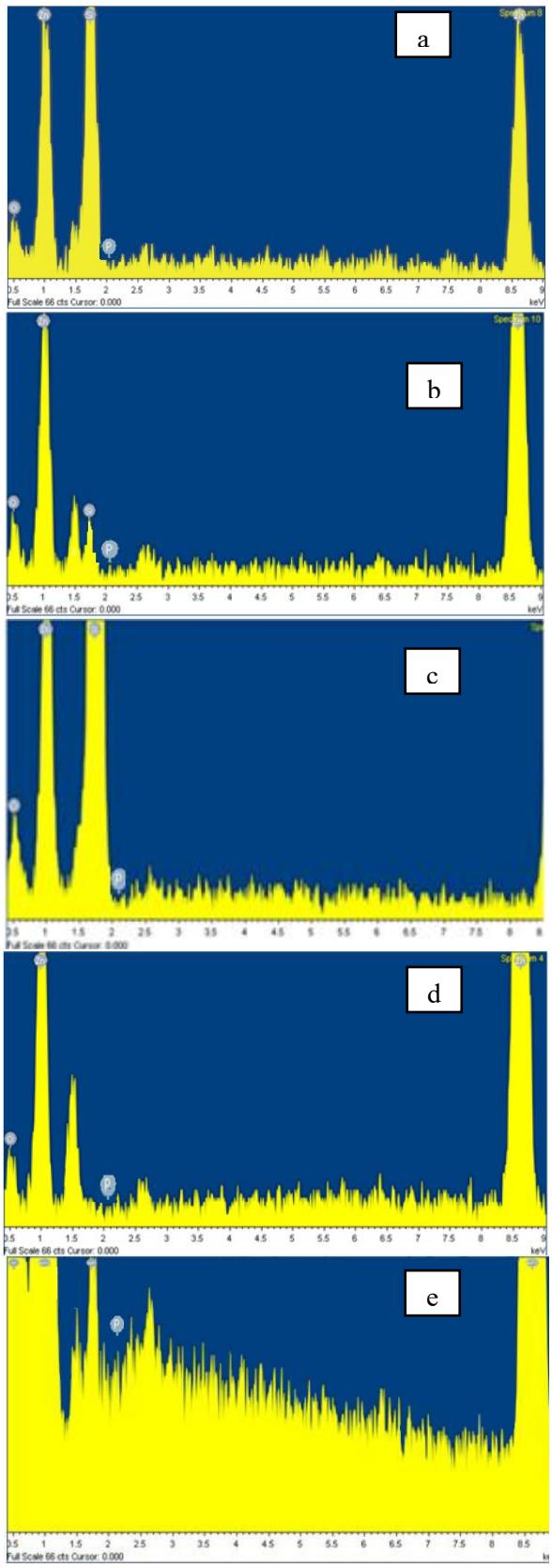

Fig. 6 EDX spectrum of sample 1 irradiated with phosphorous dose of $1x10^{14}$ ions/cm^2 6(a), EDX spectrum of sample 2 irradiated with phosphorous dose of $5x10^{14}$ ions/cm^2 6 (b), EDX spectrum of sample 3 irradiated with phosphorous dose of $1x10^{15}$ ions/cm^2 6 (c), EDXspectrum of sample 4 irradiated with phosphorous dose of $2.5x10^{15}$ ions/cm^2 6(d), EDX spectrum of sample 5 irradiated with phosphorous dose of $5x10^{15}$ ions/cm^2 6(e).

The elemental compositional analysis of irradiated ZnO-T samples (1-5) was studied by EDX. For sample 1, 2, 3, 4, and 5 EDX spectra are shown in Fig. 6. In these spectra, the Zn, O, P, and Si peaks were observed in the samples. Si content is due to the presence of Si substrate and P content was present in all samples as reported earlier in 2012 [38] where P peak was observed at 2.013 keV. This reveals that the incorporation of phosphorous ions into the zinc oxide nanotetrapods.

4. Conclusions

Results show that before and after phosphorous irradiation no changes were observed in ZnO-tetrapods samples (sample 1-5). The shape of ZnO-tetrapods samples was the same in both cases. Photoluminescence results show that before phosphorous irradiation the PL spectrum has only two peaks related to band edge (3.28 eV) and deep level emission (2.85 eV). After irradiation near band emission and deep level emission was seen, these emission peaks increase with increasing dose value. At low doses, weak peaks were observed, but at high doses strong near band emission peaks were observed. These emission peaks are defects related peaks due to phosphorous atom, called phosphorous related acceptor transition. The emission peaks at 3.31 eV and 3.34 eV can be ascribed to the free electrons to neutral-acceptor (FA) transition and acceptor bound excitation (A0 X) respectively. Both donor and acceptor states in ZnOnanotetrapods samples were seen due to the amphoteric nature of phosphorous. Energy dispersive x-ray spectroscopy results show that Zn, O, and P contents are present in the sample.

Acknowledgment

Special thanks to the University of Azad Jammu and Kashmir, Muzaffarabad for synthesis and characterization facility, and National Centre for Physics (NCP), Quaid.i.Azam University Islamabad for providing Pelletron Tendom accelerator facility.

References

[1] C. H. Ahn, Y. Y. Kim, S. W. Kang, and H. K. Cho, "Phosphorus-doped ZnO films grown nitrogen ambience by magnetron sputtering on sapphire substrates," *Phys. B Condens. Matter*, **401–402**, 370–373, (2007).

[2] X. Fang *et al.*, "P-doped ZnO Nanoparticals Synthesized by Thermal Decomposition," *Integr. Ferroelectr.*, **137**,143–148, (2012).

[3] Z.-G. Chen *et al.*, "Preparation of high purity ZnO nanobelts by thermal evaporation of ZnS.," *J. Nanosci. Nanotechnol.*, **6**, 704–707, (2006).

[4] E. Bacaksiz, M. Parlak, M. Tomakin, A. Özçelik, M. Karakız, and M. Altunbaş, "The effects of zinc nitrate, zinc acetate and zinc chloride precursors on investigation of structural and optical properties of ZnO thin films," *J. Alloys Compd.*, **466**, 447–450, (2008).

[5] A. Kołodziejczak-Radzimska and T. Jesionowski, "Zinc Oxide-From Synthesis to Application: A Review," *Mater. (Basel, Switzerland)*, **7**, 2833–2881, (2014).

[6] Y. C. Kong, D. Yu, B. Zhang, W. Fang, and S.-Q. Feng, "Ultraviolet-Emitting ZnO Nanowires Synthesized by a Physical Vapor Deposition Approach," *Appl. Phys. Lett.*, **78**, 407–409, (2001).

[7] M. Huang, Y. Wu, H. N. Feick, N. Trần, and P. D. Yang, "Catalytic Growth of Zinc Oxide Nanowires by Vapor Transport," *Adv. Mater.*, **13**, 113–116, (2001).

[8] S. C. Lyu *et al.*, "Low temperature growth and photoluminescence of well-aligned zinc oxide nanowires," *Chem. Phys. Lett.*, **363**, 134–138, (2002).

[9] W. I. Park, G.-C. Yi, M. Kim, and S. J. Pennycook, "ZnO Nanoneedles Grown Vertically on Si Substrates by Non-Catalytic Vapor-Phase Epitaxy," *Adv. Mater.*, **14**, 1841–1843, (2002).

[10] P.-X. Gao, Y. Ding, and Z. Wang, "Crystallographic Orientation-Aligned ZnO Nanorods Grown by a Tin Catalyst," *Nano Lett. - NANO LETT*, **3**, (2003).

[11] P. Gao and Z. L. Wang, "Self-Assembled Nanowire–Nanoribbon Junction Arrays of ZnO," *J. Phys. Chem. B*, **106**, 12653–12658, (2002).

[12] J. Y. Lao, J. Y. Huang, D. Z. Wang, and Z. F. Ren, "ZnO Nanobridges and Nanonails," *Nano Lett.*, **3**, 235–238, (2003).

[13] Y. Hang Leung, A. B. Djurišić, J. Gao, M. H. Xie, and W. K. Chan, "Changing the shape of ZnO nanostructures by controlling Zn vapor release: from tetrapod to bone-like nanorods," *Chem. Phys. Lett.*, **385**, 155–159, (2004).

[14] V. A. L. Roy, A. B. Djurišić, W. K. Chan, J. Gao, H. F. Lui, and C. Surya, "Luminescent and structural properties of ZnO nanorods prepared under different conditions," *Appl. Phys. Lett.*, **83**, 141–143, (2003).

[15] W. Yu, X. Li, and X. Gao, "Self-Catalytic Synthesis and Photoluminescence of ZnO Nanostructures on ZnO Nanocrystal Substrates," *Appl. Phys. Lett.*, **84**, 2658–2660, (2004).

[16] A. Umar and Y.-B. Hahn, "Large-quantity synthesis of ZnO hollow objects by thermal evaporation: Growth mechanism, structural and optical properties," *Appl. Surf. Sci. - APPL SURF SCI*, **254**, 3339–3346, (2008).

[17] Y. Zhang, H. Zhang, X. Li, L. Dong, and X. Zhong, "Mn-doped ZnO nanonails and their magnetic properties," *Nanotechnology*, **21**, 95606, (2010).

[18] J. Karamdel, C. F. Dee, and B. Majlis, "Effects of Annealing Conditions on the Surface Morphology and Crystallinity of Sputtered ZnO Nano Films," *Sains Malaysiana*, **40**, 209–213, (2011).

[19] F.-Q. He and Y.-P. Zhao, "Growth of ZnO nanotetrapods with hexagonal crown," *Appl. Phys. Lett.*, **88**, 193113, (2006).

[20] A. Janotti and C. G. de Walle, "Native point defects in ZnO," *Phys. Rev. B*, **76**, 165202, (2007).

[21] K. Tang, S.-L. Gu, J.-D. Ye, S.-M. Zhu, R. Zhang, and Y.-D. Zheng, "Recent progress of the native defects and p-type doping of zinc oxide," *Chinese Phys. B*, **26**, 47702, (2017).

[22] R. Vidya *et al.*, "Energetics of intrinsic defects and their complexes in ZnO investigated by density functional calculations," *Phys. Rev. B*, **83**, 45206, (2011).

[23] H.-J. Jin, M.-J. Song, and C.-B. Park, "A novel phenomenon: p-Type ZnO:Al films deposited on n-Si substrate," *Phys. B Condens. Matter*,. **404**, 1097–1101, (2009).

[24] L. Vines, J. Wong-Leung, C. Jagadish, E. V Monakhov, and B. G. Svensson, "Ion implantation induced defects in ZnO," *Phys. B Condens. Matter*, **407**, 1481–1484, (2012).

[25] K. E. Knutsen *et al.*, "Zinc vacancy and oxygen interstitial in ZnO revealed by sequential annealing and electron irradiation," *Phys. Rev. B*, **86**,121203, (2012).

[26] A. Sarkar *et al.*, "Defects in 6 MeV H+irradiated hydrothermal ZnO single crystal," *J. Phys. Condens. Matter*, **25**, 385501, (2013).

[27] S. Bayan and D. Mohanta, "Effect of 80-MeV nitrogen ion irradiation on ZnO nanoparticles: Mechanism of selective defect related radiative emission features," *Nucl. Instruments Methods Phys. Res. Sect. B Beam Interact. with Mater. Atoms*, **269**, 374–379, (2011).

[28] A. Ishaq *et al.*, "Effect for hydrogen, nitrogen, phosphorous, and argon ions irradiation on ZnO NWs," *J. Nanoparticle Res.*, **15**, 1467, (2013).

[29] R. Herrmann, F. J. García-García, and A. Reller, "Rapid degradation of zinc oxide nanoparticles by phosphate ions," *Beilstein J. Nanotechnol.*, **5**, 2007–2015, (2014).

[30] X. J. Wang, W. M. Chen, F. Ren, S. Pearton, and I. A. Buyanova, "Effects of P implantation and post-implantation annealing on defect formation in ZnO," *J. Appl. Phys.*, **111**, 43520, (2012).

[31] C.-C. Lin, S.-Y. Chen, and S.-Y. Cheng, "Physical characteristics and photoluminescence properties of phosphorous-implanted ZnO thin films," *Appl. Surf. Sci. - APPL SURF SCI*, **238**, 405–409, (2004).

[32] V. Vaithianathan, S. Hishita, J. Y. Park, and S. S. Kim, "Photoluminescence in phosphorous-implanted ZnO films," *J. Appl. Phys.*, **102**, 86107, (2007).

[33] Y. K. Mishra and R. Adelung, "ZnO tetrapod materials for functional applications," *Mater. Today*,**21**, 631–651, (2018).

[34] L. Zanotti, D. Calestani, M. Villani, M. Zha, A. Zappettini, and C. Paorici, "Vapour-phase growth, purification and large-area deposition of ZnO tetrapod nanostructures," *Cryst. Res. Technol.*,**45**, 667–671, (2010).

[35] F. Liu, P. J. Cao, H. R. Zhang, J. Q. Li, and H. J. Gao, "Controlled self-assembled nanoaeroplanes, nanocombs, and tetrapod-like networks of zinc oxide," *Nanotechnology*, **15**, 949–952, (2004).

[36] C. Ronning, N. G. Shang, I. Gerhards, H. Hofsäss, and M. Seibt, "Nucleation mechanism of the seed of tetrapod ZnO nanostructures," *J. Appl. Phys.*, **98**, 1–6, (2005).

[37] D.-K. Hwang *et al.*, "Study of the photoluminescence of phosphorus-doped p-type ZnO thin films grown by radio-frequency magnetron sputtering," *Appl. Phys. Lett.*, **86**,. 151917, (2005).

[38] J. Karamdel *et al.*, "Synthesis and characterization of well-aligned catalyst-free phosphorus-doped ZnO nanowires," *J. Alloys Compd.*, **512**, 68–72, (2012).